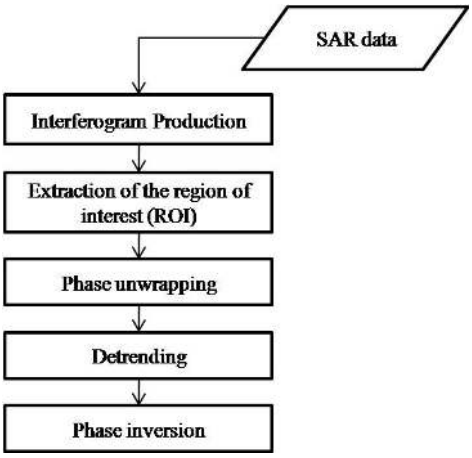

Figure A1. InSAR processing chain used in this study.

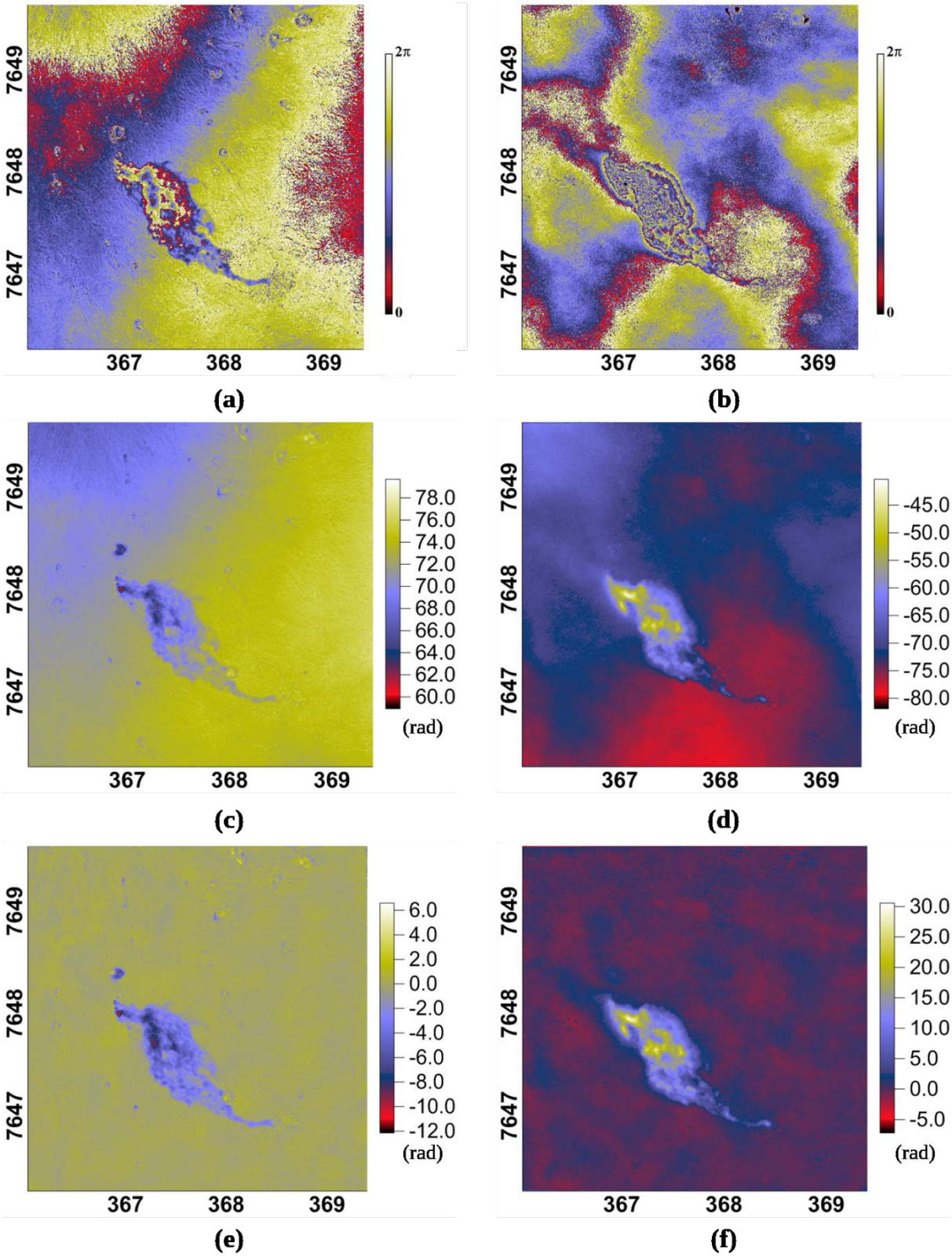

Figure A2. a.) The phase map of 20111103_20111119 from an ascending pass (angle of incidence, α_i= 40.1292°) that spans 16 days (November 03-19, 2011), centered on the location of the October 2010 lava flow. A decreasing Earth-satellite distance can be observed within the area of the lava flow (fringe pattern from the periphery is yellow-blue-red). b.) Ascending interferogram 20110303_20111013 (α_i = 48.8509°) covering 224 days (March 03, 2011 to October 13, 2011). Here an increasing Earth-satellite distance is clear (fringe pattern is red-blue-yellow) within the area of the lava flow. c.) Unwrapped phase of 20111103_20111119 in (a). d.) Unwrapped phase of 20110303_20111013 in (b). e) Detrended phase of 20111103_20111119 in (c). f) Detrended phase of 20110303_20111013 in (d). All the images are in UTM km coordinates.

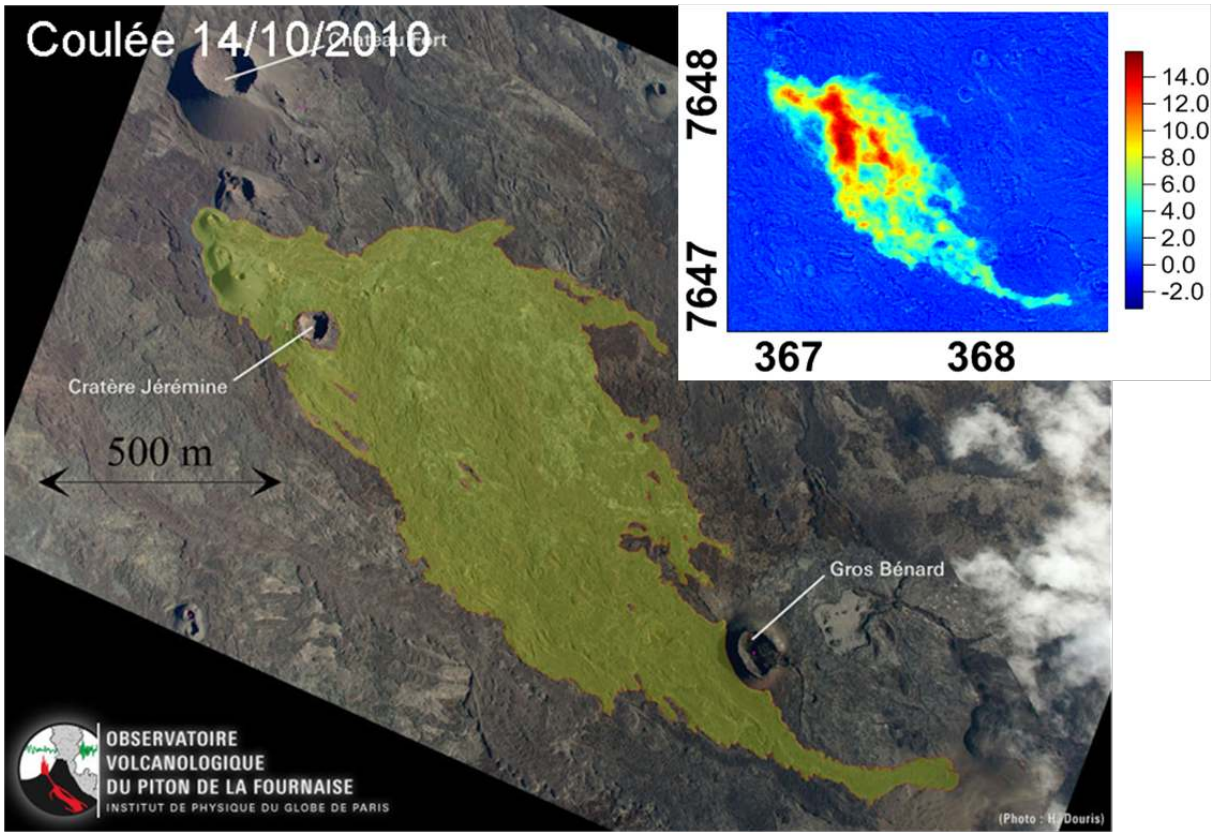

Figure A3. The emplacement of the October 2010 lava flow on Piton de la Fournaise, as mapped by the OVPF following an aerial survey. The inset is the CSK-derived thickness map illustrating a similar shape and extent for the lava flow. Clearly, the advantage of the InSAR map is that it not only provides a spatial view of the flow but it can also provide a 3D perspective and a good estimate of the volume.

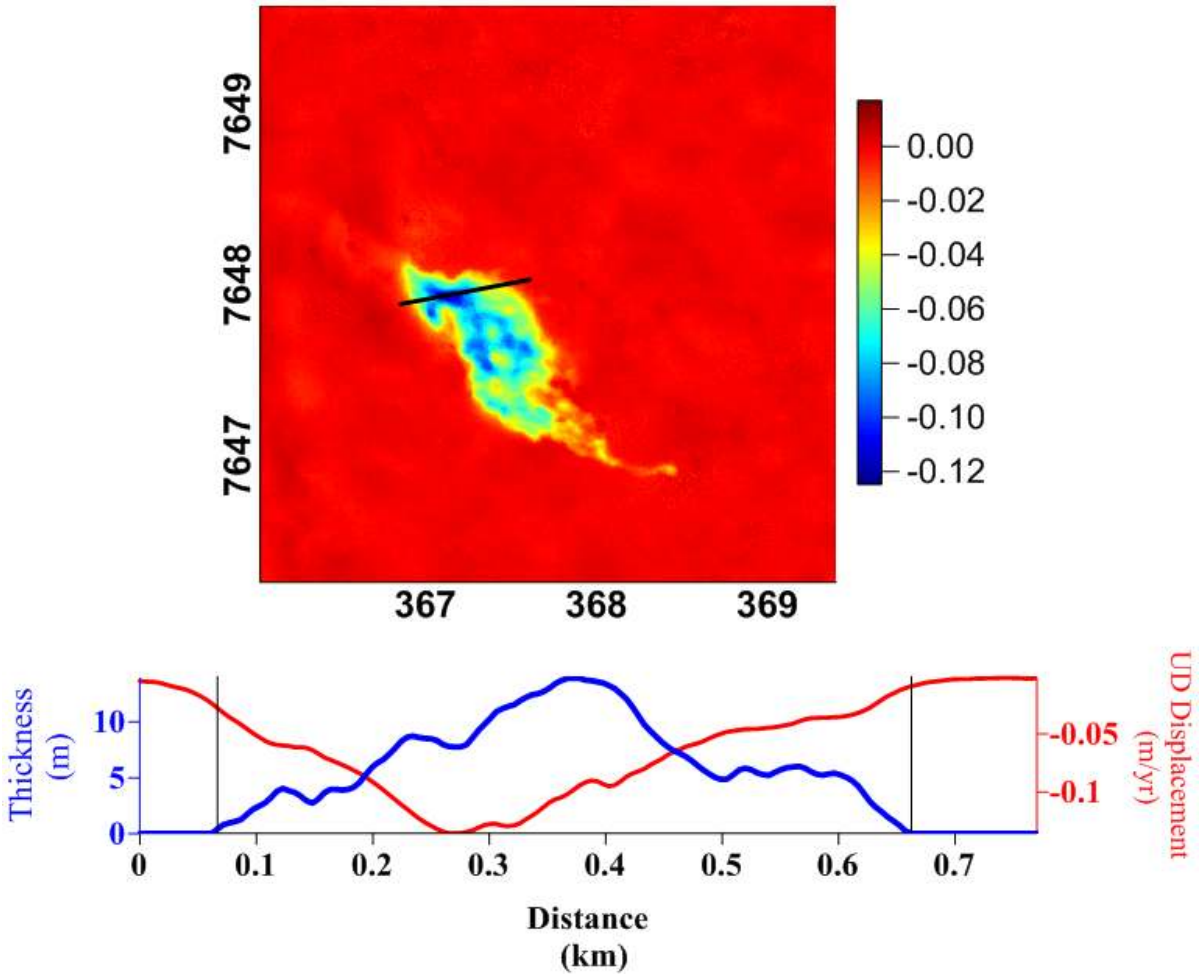

Figure A4. The cross-section of the thickness (red line) and the vertical displacement map (blue line). The two gray vertical lines correspond to the edge of the subsidence area of the lava flow. Here the subsidence extends beyond the lava flow limits. Although low, the subsidence is clearly visible for at least 100 m beyond the lava flow on the left-hand side. This reflects the flexion of the substratum under the loading and compaction of the lava flow. This phenomenon was first identified by [Murray, 1988].

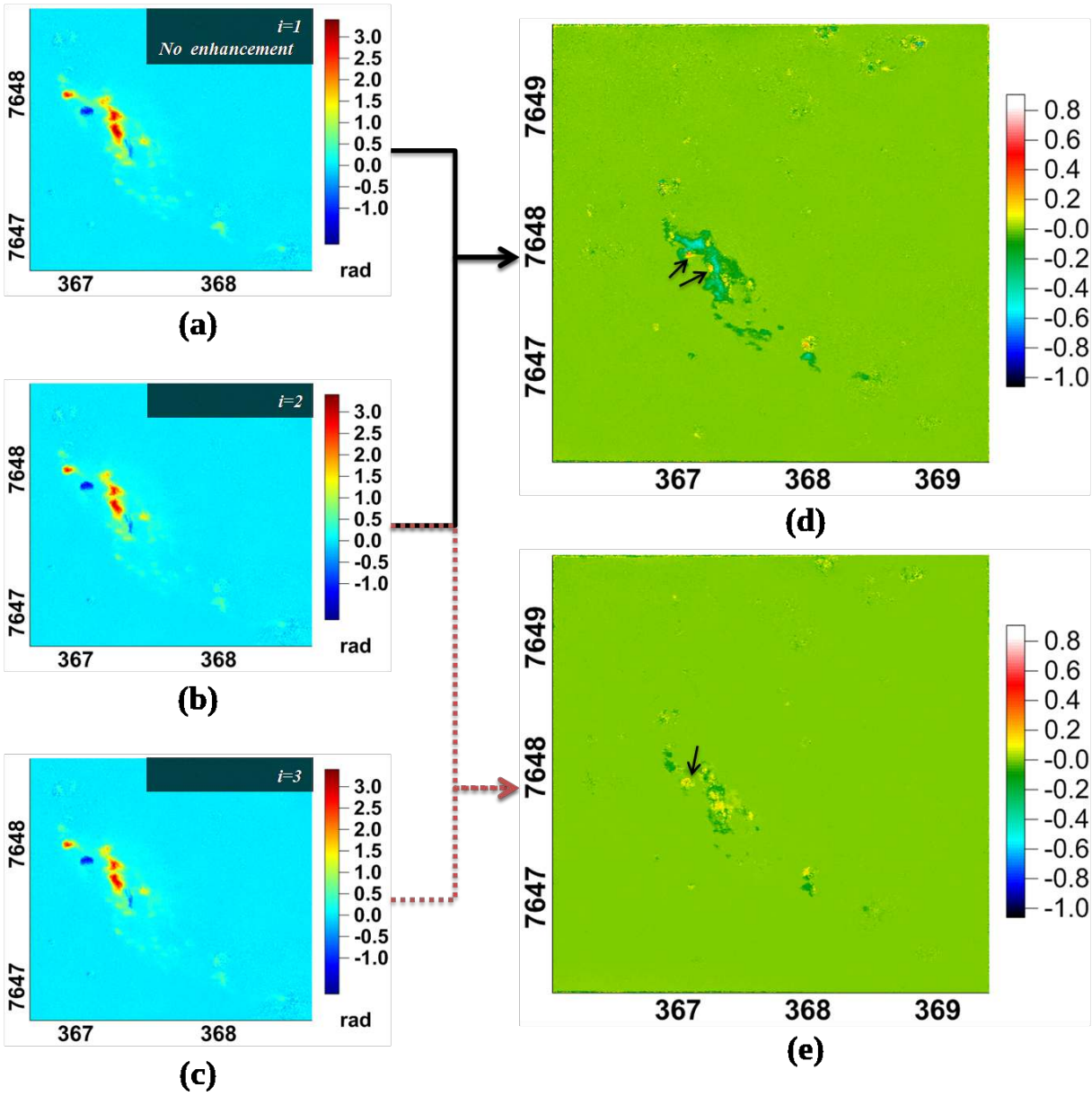

Figure A5. The resulting residual maps (ε-map) after applying the low-pass filter. (a) The ε-map prior to enhancement. (b) The ε-map after the first application of the low-pass filter. (c) The ε-map after the second application of the low-pass filter. (d) The difference between (a) and (b), with respect to (b). Note that we have decreased the residual values as shown by the negative values within the area of the lava flow. However, as marked by the arrows, we may also have induced residuals during the application of the low-pass filter. This can also be observed in (e) as we mapped the difference between the third iteration and the second iteration residuals. All the images are in UTM km coordinates.

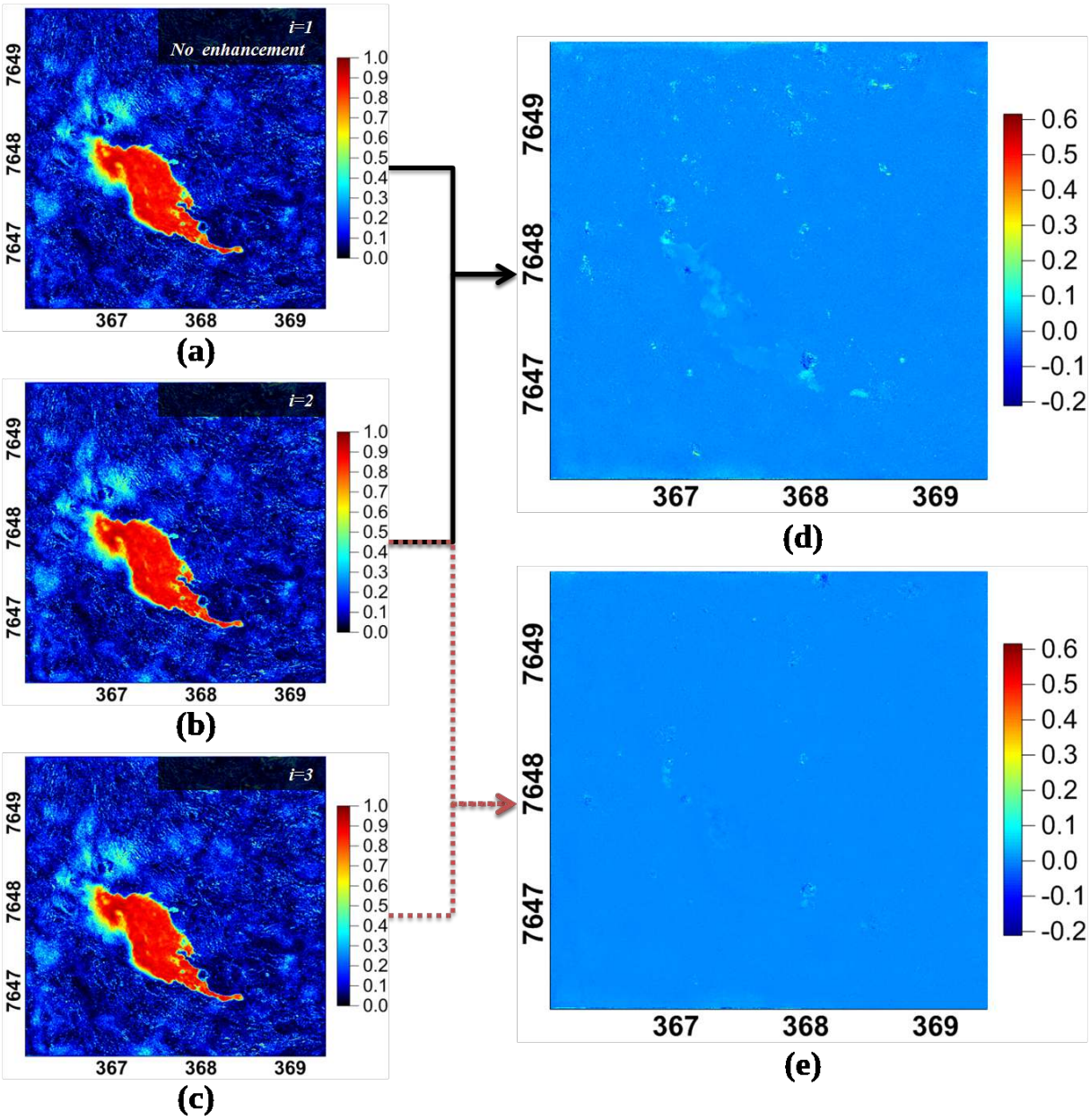

Figure A6. The resulting r^2-map after the application of the low-pass filter. A value closer to 1.0 means a better agreement of the inversion model to the actual data. (a) The r^2-map prior to enhancement. (b) The resulting r^2-map after the first application of the low-pass filter. (c). The resulting r^2-map after the second application of the low-pass filter. (d) The difference between (a) and (b), with respect to (b). Note that we have improved the map of the goodness-of-fit mostly within the area of the lava flow. (e) The difference between (b) and (c), with respect to (c). All the images are in UTM km coordinates.